

See discussions, stats, and author profiles for this publication at: <https://www.researchgate.net/publication/6373148>

# HPLC-ESI+-MS/MS analysis of N7-guanine-N7-guanine DNA cross-links in tissues of mice exposed to 1,3-butadiene.

ARTICLE *in* CHEMICAL RESEARCH IN TOXICOLOGY · JUNE 2007

Impact Factor: 3.53 · DOI: 10.1021/tx700020q · Source: PubMed

CITATIONS

29

READS

12

## 6 AUTHORS, INCLUDING:



Vernon Walker

University of Vermont

101 PUBLICATIONS 3,042 CITATIONS

SEE PROFILE



Jeffrey K Wickliffe

Tulane University

71 PUBLICATIONS 865 CITATIONS

SEE PROFILE



Natalia Tretyakova

University of Minnesota Twin Cities

104 PUBLICATIONS 2,362 CITATIONS

SEE PROFILE

## HPLC–ESI<sup>+</sup>-MS/MS Analysis of *N*7-Guanine–*N*7-Guanine DNA Cross-Links in Tissues of Mice Exposed to 1,3-Butadiene

Melissa Goggin, Rachel Loeber, Soobong Park, Vernon Walker,<sup>†</sup> Jeffrey Wickliffe,<sup>‡</sup> and Natalia Tretyakova\*

Cancer Center and Department of Medicinal Chemistry, University of Minnesota, Minneapolis, Minnesota 55455

Received January 16, 2007

1,3-Butadiene (BD) is a major industrial chemical used in rubber and plastics production and is recognized as an animal and human carcinogen. Although the exact mechanism of BD-induced carcinogenesis is unknown, chemical reactions of epoxide metabolites of BD with DNA to form nucleobase adducts are likely to contribute to multistage carcinogenesis. Among BD-derived epoxy metabolites, 1,2:3,4-diepoxybutane (DEB) appears to be the most genotoxic and carcinogenic, probably because of its bifunctional nature. Initial DNA alkylation by DEB produces *N*7-(2'-hydroxy-3',4'-epoxybut-1'-yl)-guanine monoadducts, which can then be hydrolyzed to *N*7-(2',3',4'-trihydroxy-1'-yl)guanine or can react with another site in double-stranded DNA to form 1,4-bis(guan-7-yl)-2,3-butanediol (bis-*N*7G-BD) cross-links. While (2',3',4'-trihydroxy-1'-yl)guanine lesions have been previously quantified *in vivo*, they cannot be used as a biomarker of DEB because the same lesions are also formed by another, more prevalent BD metabolite, 1,2-epoxy-3,4-butanediol. In contrast, bis-*N*7G-BD can only be formed from DEB, potentially providing a specific biomarker of DEB formation. We have developed a quantitative HPLC–ESI<sup>+</sup>-MS/MS method for measuring racemic and *meso* forms of bis-*N*7G-BD in DNA extracted from tissues of BD-exposed laboratory animals. In our approach, bis-*N*7G-BD adducts are released from DNA as free bases by neutral thermal hydrolysis, purified by solid-phase extraction, and subjected to HPLC–ESI<sup>+</sup>-MS/MS analysis. Selected reaction monitoring is performed by following the loss of a guanine moiety from protonated molecules of bis-*N*7G-BD and the formation of protonated guanine under collision-induced dissociation. Quantitative analysis of racemic and *meso* forms of bis-*N*7G-BD is based on isotope dilution with the corresponding <sup>15</sup>N-labeled internal standards. The lower limit of quantification of our current method is 10–20 fmol/0.1 mg of DNA. The accuracy and precision of the new method were determined by spiking control mouse liver DNA with racemic and *meso* forms of bis-*N*7G-BD (10 fmol each), followed by sample processing and HPLC–ESI<sup>+</sup>-MS/MS analysis. Calculated amounts of racemic and *meso* forms of bis-*N*7G-BD were within 20% of the theoretical value ( $9.7 \pm 2$  and  $9.2 \pm 1.9$  fmol, respectively,  $N = 4$ ). DNA extracted from liver and lung tissues of mice exposed to 625 ppm butadiene for 5 days contained  $3.2 \pm 0.4$  and  $1.8 \pm 0.5$  racemic adducts per  $10^6$  guanines, respectively, while the amounts of *meso*-bis-*N*7G-BD were below the detection limits of our method (1 per  $10^7$  guanines). Control animals did not contain either bis-*N*7G-BD lesion. Sensitive and specific quantitative methods for bis-*N*7G-BD analysis developed in this work provide a unique biomarker of DEB-induced DNA alkylation following exposure to BD.

### Introduction

1,2:3,4-Diepoxybutane (DEB)<sup>1</sup> (Scheme 1) is an important metabolite of 1,3-butadiene (BD), an industrial chemical and an environmental pollutant found in automobile exhaust and in cigarette smoke (1, 2). BD is classified as “reasonably anticipated to be a human carcinogen” (U.S. Department of Health and Human Services) on the basis of its multisite carcinogenicity in laboratory animals and its pronounced genotoxic effects, including the induction of point mutations, large deletions, and chromosomal aberrations (3–8). In chronic inhalation experi-

ments with B6C3F1 mice and Sprague–Dawley rats, BD was carcinogenic in both species (8, 9). However, while mice developed tumors after chronic exposure to as little as 6.25 ppm BD (8), much higher concentrations (1000 ppm) were required to induce tumors in rats (9). Furthermore, the target tissues for BD-induced cancer in mice (lung, heart, hematopoietic system) are different from those in rats (thyroid, pancreas, testis for males, uterus for females) (8, 9). These interspecies differences in sensitivity have been attributed to differences in BD metabolism in mice and rats, in particular, the increased formation of DEB and other DNA-reactive metabolites in the mouse (10).

BD requires metabolic activation before it can exert its biological effects (11). *In vivo* metabolism of BD to DEB is catalyzed by cytochrome P450 2E1 and P450 2A6 monooxygenases (12–14). The first epoxidation step yields (*R*)- and (*S*)-3,4-epoxy-1-butene (EB) (12, 13) (Scheme 1). EB can then be hydrolyzed to 1-butene-3,4-diol or can undergo a second oxidation to yield (*R,R*)-, (*S,S*)-, and *meso*-DEB (14) (Scheme 1).

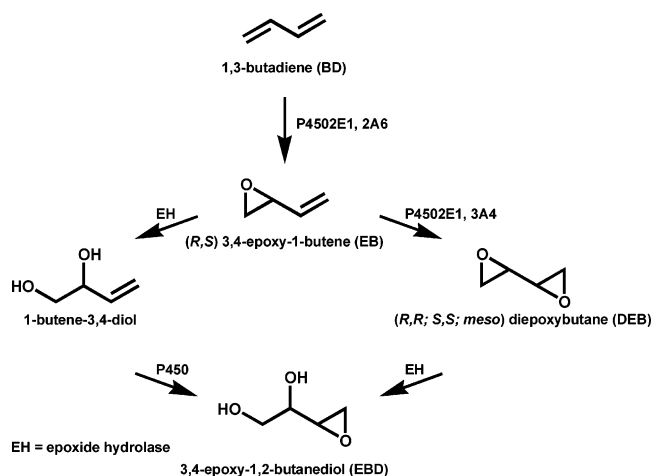
\* To whom correspondence should be addressed. Phone: (612) 626-3432. E-mail: trety001@umn.edu.

<sup>†</sup> Lovelace Respiratory Research Institute, Albuquerque, NM.

<sup>‡</sup> University of Texas Medical Branch, Galveston, TX.

<sup>1</sup> Abbreviations: BD, 1,3-butadiene; bis-*N*7G-BD, 1,4-bis(guan-7-yl)-2,3-butanediol; DEB, 1,2:3,4-diepoxybutane; EB, 3,4-epoxy-1-butene; EBD, 3,4-epoxy-1,2-butanediol; EH, epoxide hydrolase; HPLC–ESI<sup>+</sup>-MS/MS, liquid chromatography–electrospray ionization tandem mass spectrometry; SD, standard deviation; SRM, selected reaction monitoring; THBG, *N*7-(2',3',4'-trihydroxy-1'-yl)guanine.

## Scheme 1. Metabolism of BD to DNA-Reactive Species



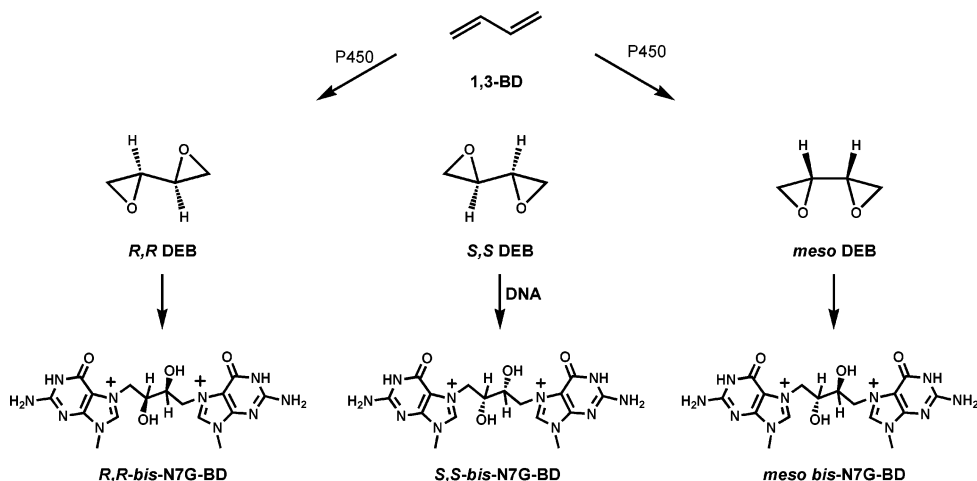
Although DEB is a relatively minor metabolite of BD, experimental evidence suggests that it is responsible for many of the adverse effects of BD. DEB is 50–100-fold more genotoxic and mutagenic in human cells *in vitro* than its monoepoxide analogues EB and 3,4-epoxy-1,2-butanediol (EBD) (15, 16). Efficient metabolism of BD to DEB in target tissues of laboratory mice is thought to cause the increased susceptibility of this species to BD carcinogenesis (10). The widespread human exposure to BD, as well as its potent carcinogenic effects, warrants further investigation of the origins of interspecies differences in susceptibility to BD carcinogenesis.

While all three DEB stereoisomers are generated metabolically (14), biological studies reveal significant differences between the ability of (*R,R*)-, (*S,S*)-, and *meso*-DEB to inactivate T7 coliphage (17), induce chromosomal aberrations (18), and cause mutagenesis in maize (19). Among the three stereoisomers, (*S,S*)-DEB exhibits the most potent genotoxicity and cytotoxicity, followed by (*R,R*)- and then *meso*-DEB (17–19). Furthermore, DEB stereoisomers induce different spectra of mutations in the *supF* gene, suggesting stereospecific differences between the formation and/or repair of DNA adducts induced by the optical isomers of DEB (20).

The genotoxicity and cytotoxicity of DEB are thought to result from its ability to form bifunctional DNA adducts by sequentially alkylating two nucleophilic sites within the DNA duplex. DNA–DNA cross-linking by DEB was first discovered by Lawley and Brooks in the 1960s (21). These authors isolated *N7*-guanine–*N7*-guanine adducts from DEB-treated salmon

sperm DNA (21). More recently, our laboratory employed modern spectroscopic methods to determine the chemical structure of these lesions, which were identified as 1,4-bis(guan-7-yl)-2,3-butanediol (bis-*N7G*-BD) (Scheme 2) (22). Lawley and Brooks noted that DEB-treated DNA renatured more rapidly than control DNA, suggesting that interstrand DNA–DNA cross-links of DEB were formed (21). This was further confirmed by gel electrophoresis experiments of Millard and White (23). Interestingly, a strong sequence preference for interstrand DNA cross-linking between the *N7* positions of distal guanine nucleobases within the 5'-GNC-3' context was observed both in synthetic oligomers and in chromatinized restriction fragments (24–27). More recently, stable isotope labeling was employed to demonstrate that DEB produced both inter- and intrastrand cross-links (27). While the *S,S* isomer specifically gave rise to interstrand lesions, *meso*-DEB induced equal numbers of intrastrand and interstrand cross-links (27). These findings are consistent with the greater cytotoxic effect of (*S,S*)-DEB (17–19). In addition to guanine–guanine lesions, DEB can form adenine–guanine cross-links, e.g., 1-(aden-1-yl)-4-(guan-7-yl)-2,3-butanediol, 1-(aden-3-yl)-4-(guan-7-yl)-2,3-butanediol, 1-(aden-7-yl)-4-(guan-7-yl)-2,3-butanediol, and 1-(aden-*N*<sup>6</sup>-yl)-4-(guan-7-yl)-2,3-butanediol (28), exocyclic DNA lesions (29) (Antsyovich et al., unpublished data), and 2',3',4'-trihydroxybut-1'-yl adducts that result from hydrolysis of one of the two epoxy groups of DEB. The bis-*N7G*-BD cross-links appear to be the most abundant bifunctional DNA lesions in DEB-treated DNA (22, 28).

Because of the proposed key role of DNA–DNA cross-links of DEB in mutagenesis and carcinogenesis of BD, there is an urgent need for a specific biomarker of their formation and repair (30). Previous studies have analyzed *N7*-(2',3',4'-trihydroxy-1'-yl)guanine (THBG) adducts in DNA of BD-treated laboratory animals (31–33). However, THBG lesions cannot be used as specific biomarkers of BD metabolism to DEB, because they are also formed by another, more prevalent metabolite of BD, EBD (Scheme 1) (32, 33). In the present work, HPLC–ESI<sup>+</sup>-MS/MS methods for quantitative analyses of bis-*N7G*-BD were developed and validated. These methods were used to analyze DEB-induced DNA–DNA cross-links in tissues of laboratory mice exposed to BD by inhalation. Our methods provide the first DEB-specific DNA biomarker available for studies of bifunctional DEB–DNA adduct formation and repair *in vivo*.

Scheme 2. Formation of Stereoisomeric Bis-*N7G*-BD Adducts upon Exposure to BD

## Experimental Procedures

**Caution:** DEB is a suspected human carcinogen and must be handled with adequate safety precautions.

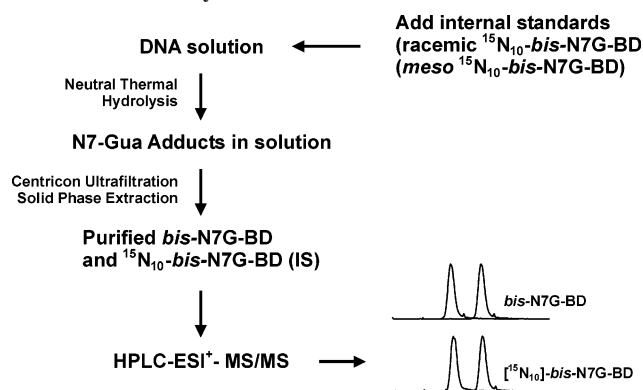
**Materials and Methods.** All solvents and chemicals were obtained from Sigma-Aldrich (Milwaukee, WI, St. Louis, MO) unless specified otherwise. Racemic DEB and calf thymus DNA were purchased from Sigma-Aldrich. Phase lock gels were from Fisher Scientific (Waltham, MA), and Tris-saturated phenol was from Roche Applied Science (Indianapolis, IN). Bis-N7G-BD stereoisomers and their  $^{15}\text{N}_{10}$  analogues were prepared at our laboratory as described previously (22, 27). HPLC–ESI–MS/MS confirmed that the residues of unlabeled adduct in standard solutions were <0.2%. Stock solutions of racemic and *meso* forms of bis-N7G-BD and their internal standards were prepared in 0.1 N HCl (20–30  $\mu\text{M}$ ) and stored at  $-20^\circ\text{C}$ . The concentrations were periodically checked by UV spectrophotometry ( $\epsilon_{252} = 15\,700$  at pH 1) and HPLC–ESI–MS/MS. Standard solutions were prepared from stock solutions by serial dilutions with 0.1 N HCl and stored at  $-20^\circ\text{C}$ .

**Animals and Treatment.** C57BL/6 mice were exposed to 625 ppm BD by inhalation for 5 days (7 h/day) at the Department of Preventive Medicine and Community Health at the University of Texas Medical Branch. All procedures were carried out in accordance with UTMB ACUC protocol 880202401. Mice were exposed in Hinners-type stainless steel chambers (0.85  $\text{L}/\text{m}^3$ ) to approximately 625 ppm BD for 7 h/day for 5 days (30 air volume changes/h). The temperature and humidity were maintained at  $24 \pm 1^\circ\text{C}$  and  $50 \pm 5\%$ , respectively. During exposure, the animals were housed in individual stainless steel wire mesh cages within the chambers to ensure uniform delivery of the gas-phase BD. BD, from a 99% pure source (Scott Specialty Gases, Pasadena, TX), was metered through a mass flow controller to achieve the desired concentration. Chamber concentrations were continuously monitored using gas chromatography (GC) and photoionization detection. Chamber atmospheres were continuously drawn through the GC sample loop and periodically introduced into the flow of  $\text{N}_2$  carrier gas using a computer-controlled, air-actuated valve. The concentration of BD was calculated by integrating the peak areas. The GC was calibrated at the beginning of each day using a 60 ppm BD certified standard (Scott Specialty Gases). Air controls were maintained in identical chambers. The animals were euthanized immediately following the inhalation exposure period. Tissues including liver and lung were removed and flash frozen in liquid nitrogen. Frozen tissues were shipped on dry ice to the University of Minnesota, where they were stored in a  $-80^\circ\text{C}$  freezer until analysis.

**DNA Isolation.** The tissue was weighed (0.1–0.5 g) and homogenized in 10 mL of cold Tris–EDTA buffer. The nuclei were isolated by centrifugation at 2700 rpm for 15 min and resuspended in lysis buffer. Following addition of RNase T1 and RNase A, the lysates were incubated at  $37^\circ\text{C}$  for 1 h. Proteinase K was added, and the resulting mixture was incubated for an additional 4 h at  $37^\circ\text{C}$ . DNA was extracted using phenol/chloroform extraction and ethanol precipitation according to a previously reported methodology (34). The isolated DNA was hydrated overnight, and the solutions were homogenized by shearing through a 22 gauge needle. The amounts and purity of DNA were determined by UV spectrophotometry ( $20A_{260} = 1 \text{ mg/mL DNA}$ ). The  $A_{260}/A_{280}$  ratios were found to be between 1.7 and 1.9, ensuring minimal protein contamination. Any samples exhibiting a lower  $A_{260}/A_{280}$  ratio were re-extracted by the same procedure.

**dG Quantitation.** DNA was quantified by dG analysis in enzymatic hydrolysates. Approximately 10  $\mu\text{g}$  of each DNA sample was dissolved in 70  $\mu\text{L}$  of 10 mM ammonium acetate/1 mM  $\text{ZnCl}_2$ , pH 5.3 and digested with nuclease P1 (2.3 U) and alkaline phosphatase (10 U) at  $37^\circ\text{C}$  for 30 min. dG was quantified by HPLC–UV analysis on an Agilent Technologies model 1100 HPLC system (Wilmington, DE) incorporating a diode array detector and an autosampler. A Zorbax Eclipse XDB-C8 ( $4.6 \times 150 \text{ mm}$ ,  $5 \mu\text{m}$ ) column (Agilent Technologies, Palo Alto, CA) was eluted with a

## Scheme 3. Experimental Scheme for HPLC–ESI<sup>+</sup>–MS/MS Analysis of Bis-N7G-BD Adducts



gradient of 150 mM ammonium acetate (A) and acetonitrile (B). The solvent composition was kept at 100% A for 2.5 min, then linearly changed to 4.5% B in 19 min and further to 30% B in 3 min, and then maintained at 30% B for 5.5 min. The UV signal was monitored at 260 nm. Calibration curves were constructed by injecting known amounts of dG standard.

**Optimization of Neutral Thermal Hydrolysis.** Calf thymus DNA (500  $\mu\text{g}$ ) was treated with the racemic or *meso* form of DEB (0.129 mmol), and the DNA was precipitated with cold ethanol. Alkylated DNA was resuspended in water and heated at  $70^\circ\text{C}$  for various periods of time (3–120 min). Aliquots were removed and frozen until HPLC–ESI<sup>+</sup>–MS analysis. To determine the total number of racemic bis-N7G-BD and *meso*-bis-N7G-BD adducts in this DNA, several aliquots were analyzed following quantitative release of the cross-links by thermal hydrolysis ( $70^\circ\text{C}$  for 120 min). First-order constants ( $k$ ) were calculated from the slope of the plot of  $\ln[c/c_0] = -kt$ , where  $t$  is the incubation time,  $c$  is the concentration of bis-N7G-BD remaining in DNA at time  $t$ , and  $c_0$  is the starting concentration of bis-N7G-BD in DNA. Both adducts were quantitatively released upon heating at  $70^\circ\text{C}$  for 1 h.

**SPE Conditions.** Our original methodology employed C18 SPE cartridges; however, harsh elution conditions (0.1 N HCl) were required to elute bis-N7G-BD from the C18 packing. Therefore, we employed mixed-phase SPE cartridges that combine reversed-phase and anion-exchange chromatography separation (Oasis MAX). We found that large cartridges (500 mg capacity) were required for purification of mouse liver DNA hydrolysates (100  $\mu\text{g}$ ), since smaller cartridges (50 mg) did not have sufficient capacity for this sample size. Bis-N7G-BD cross-links were readily eluted from Oasis MAX columns with 80% methanol. Using the optimized SPE methodology, we consistently obtain 80–90% recovery of racemic bis-N7G-BD and *meso*-bis-N7G-BD standards spiked into DNA.

**DNA Hydrolysis and Sample Preparation.** DNA samples (100  $\mu\text{g}$ ) were spiked with a mixture of racemic [ $^{15}\text{N}_{10}$ ]bis-N7G-BD and *meso*-[ $^{15}\text{N}_{10}$ ]bis-N7G-BD internal standards (500 fmol each) and subjected to neutral thermal hydrolysis (1 h at  $70^\circ\text{C}$ ) to release bis-N7G-BD adducts (Scheme 3). The partially depurinated DNA was removed by Centricon YM-10 filtration (Millipore Corp., Billerica, MA). Bis-N7G-BD adducts were isolated by solid-phase extraction (SPE). Oasis MAX cartridges (500 mg, 6 mL, Waters Corp., Milford, MA) were prepared by washing with methanol (6 mL) and 0.2 N NaOH (6 mL). Samples were loaded in 0.1 N NaOH and washed with 0.01 N NaOH (6 mL), 0.01 N KOH in methanol (6 mL), water (2 mL), 1 M ammonium acetate, pH 6.8 ( $2 \times 4 \text{ mL}$ ), water (2 mL), and 5% methanol (6 mL). Bis-N7G-BD and its internal standard were eluted with 80% methanol/water (6 mL). SPE fractions containing bis-N7G-BD adducts were dried under nitrogen and dissolved in 15 mM ammonium acetate, pH 5.5 (25  $\mu\text{L}$ ), prior to analysis by HPLC–ESI<sup>+</sup>–MS/MS. The injection volume was 8  $\mu\text{L}$ .

**HPLC–ESI<sup>+</sup>–MS/MS Method.** An Agilent 1100 capillary HPLC system (Wilmington, DE) interfaced to a Thermo-Finnigan



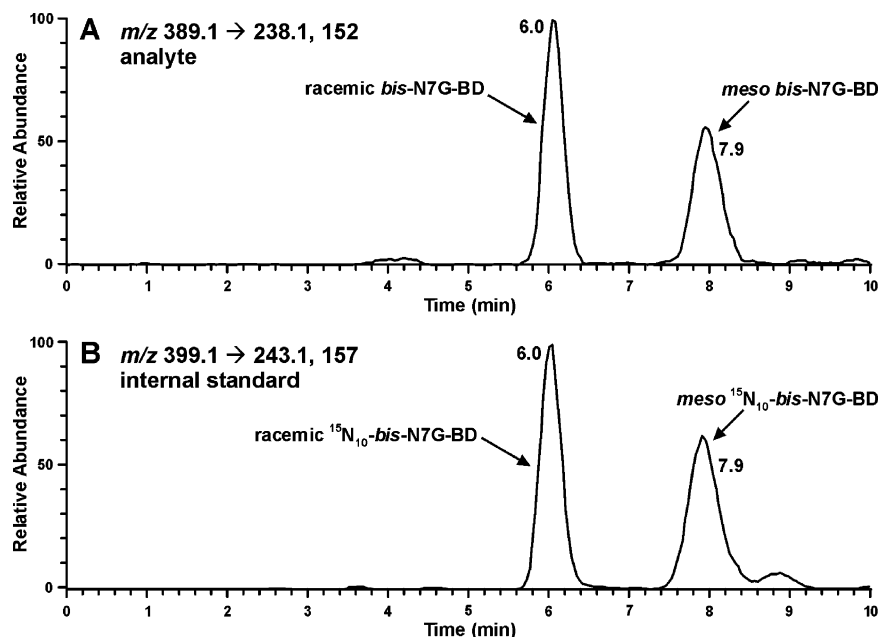


Figure 1. HPLC-ESI<sup>+</sup>-MS/MS analysis of bis-N7G-BD diastereomers (A) and their internal standards (B).

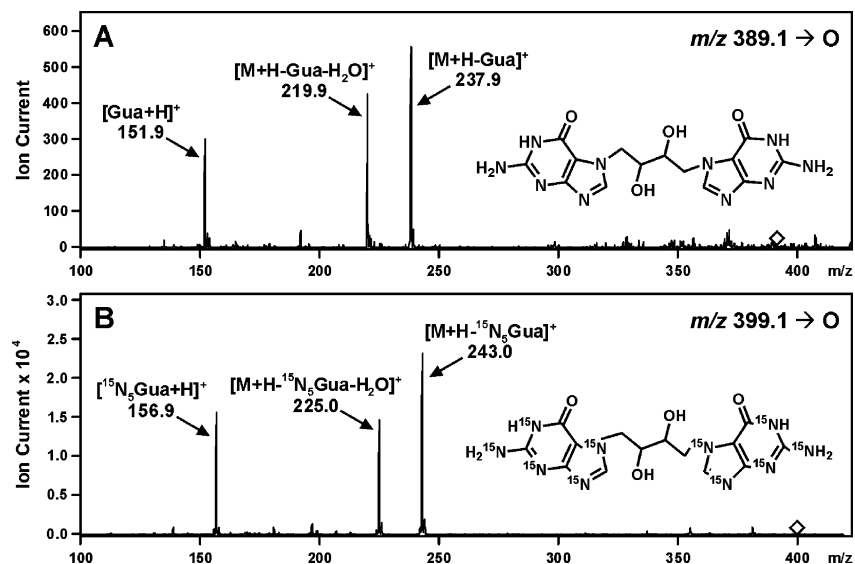


Figure 2. ESI<sup>+</sup>-MS/MS spectra of bis-N7G-BD (A) and [ $^{15}\text{N}_{10}$ ]bis-N7G-BD (B).

TSQ Quantum Ultra mass spectrometer (Thermo Fisher Scientific Corp., Waltham, MA) was used in all analyses. Chromatographic separation was achieved with a Zorbax Extend C18 column (3.5  $\mu\text{m}$ , 150  $\times$  0.5 mm) eluted isocratically with 5.2% acetonitrile in 15 mM ammonium acetate, pH 5.5. The HPLC flow rate was 12  $\mu\text{L}/\text{min}$ . The injection volume was typically 8  $\mu\text{L}$ . With this solvent system, the retention time of racemic bis-N7G-BD was 5.6–6 min, while *meso*-bis-N7G-BD eluted at 7.3–8 min (Figure 1). The mass spectrometer was operated in the positive ion mode, with nitrogen used as a sheath gas (5 L/min). Electrospray ionization was achieved at a spray voltage of 4.0 kV and a capillary temperature of 270  $^{\circ}\text{C}$ . CID was achieved with Ar as a collision gas (1.1 mTorr) and a collision energy of 10 V. The mass spectrometer parameters were optimized for maximum response during infusion of standard solutions of bis-N7G-BD.

Bis-N7G-BD lesions were quantified by isotope dilution with racemic [ $^{15}\text{N}_{10}$ ]bis-N7G-BD and *meso*-[ $^{15}\text{N}_{10}$ ]bis-N7G-BD internal standards. Quantitative analyses were performed in the selected reaction monitoring (SRM) mode using HPLC-ESI<sup>+</sup>-MS/MS peak areas corresponding to the neutral loss of guanine from protonated molecules of bis-N7G-BD ( $m/z$  389.1 [M + H]<sup>+</sup>  $\rightarrow$  238.0 [M + H - Gua]<sup>+</sup> and the formation of guanine cations ( $m/z$  389.1 [M +

H]<sup>+</sup>  $\rightarrow$  152.0 [Gua + H]<sup>+</sup>) (Figures 1 and 2). *meso*-[ $^{15}\text{N}_{10}$ ]Bis-N7G-BD and racemic [ $^{15}\text{N}_{10}$ ]bis-N7G-BD internal standards were analyzed analogously using the transitions  $m/z$  399.1 [M + H]<sup>+</sup>  $\rightarrow$  243.0 [M + H - [ $^{15}\text{N}_5$ ]Gua]<sup>+</sup> and 399.1 [M + H]<sup>+</sup>  $\rightarrow$  157.0 [[ $^{15}\text{N}_5$ ]Gua + H]<sup>+</sup> (Figures 1 and 2). Quantitative analyses were based on the ratio of the area under the peak in the selected ion chromatogram corresponding to the analyte to the peak area of the internal standard (relative response ratios). Standard curves were constructed by analyzing solutions containing 0–1000 fmol of the racemic and *meso* forms of bis-N7G-BD and 500 fmol of the racemic and *meso* forms of [ $^{15}\text{N}_{10}$ ]bis-N7G-BD, followed by regression analysis of the relative response ratios calculated from HPLC-ESI<sup>+</sup>-MS/MS peak area ratios corresponding to the analytes and their internal standards (Figure 3).

**HPLC-ESI<sup>+</sup>-MS/MS Method Validation.** The lower limits of detection (LODs) for pure bis-N7G-BD diastereomers were 1 fmol for racemic bis-N7G-BD standard and 5 fmol for *meso*-bis-N7G-BD standard, while the corresponding values for bis-N7G-BD spiked in control mouse DNA (100  $\mu\text{g}$ ) were 5 and 10 fmol, respectively. The lower limits of quantification (LOQs) of the adducts spiked in control mouse DNA (100  $\mu\text{g}$ ) were 10 fmol for racemic bis-N7G-BD and 20 fmol for *meso*-bis-N7G-BD. Method

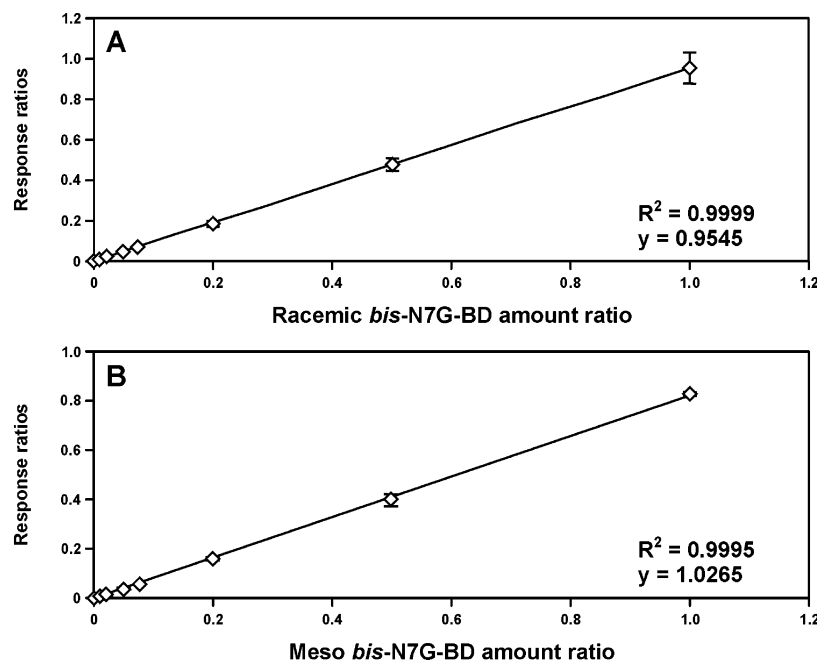


**Figure 3.** Calibration curves for HPLC–ESI<sup>+</sup>–MS/MS analysis of pure standards of racemic bis-N7G-BD (A) and *meso* bis-N7G-BD (B) by isotope dilution with [<sup>15</sup>N<sub>10</sub>]bis-N7G-BD.

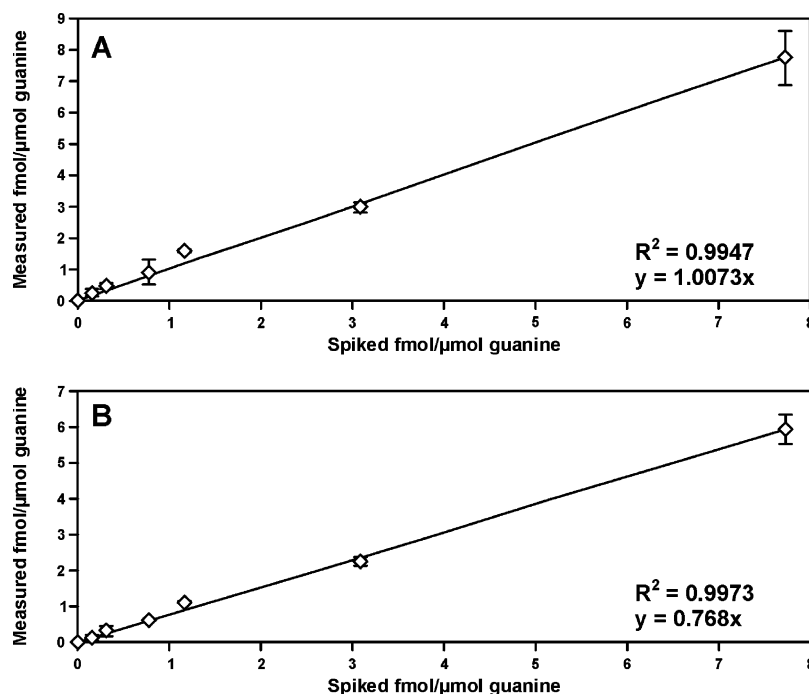


**Figure 4.** Correlation between expected and measured levels of racemic (A) and *meso* (B) forms of bis-N7G-BD in mouse liver DNA (100 µg) spiked with known amounts of bis-N7G-BD (0–500 fmol).

calibration curves were obtained by spiking mouse liver DNA (100 µg) with racemic bis-N7G-BD and *meso*-bis-N7G-BD standards (0–500 fmol) and the corresponding <sup>15</sup>N<sub>10</sub> internal standards (500 fmol) (Figure 4), followed by sample processing and HPLC–ESI–MS/MS analysis. Method accuracy was calculated from the equation  $(100C_m)/C_a$ , where  $C_m$  is the mean concentration measured and  $C_a$  is the actual concentration added. The coefficient of variation was calculated from the equation  $[100(SD)]/C_m$ , where SD is the standard deviation. Inter-run assay performance at the LOQ was investigated over three separate days.

## Results

**HPLC–MS/MS Method Development.** We have developed an HPLC–ESI<sup>+</sup>–MS/MS method to quantify bis-N7G-BD cross-

links in DNA isolated from BD-exposed laboratory animals. In our approach, DNA is spiked with <sup>15</sup>N-labeled racemic and *meso* forms of bis-N7G-BD (internal standards for mass spectrometry) and subjected to neutral thermal hydrolysis to release N7-alkylguanine adducts as free bases (Scheme 3). Following Centricon ultrafiltration to remove partially depurinated DNA, bis-N7G-BD conjugates and their internal standards are purified via solid-phase extraction on Oasis mixed mode cartridges. Quantitative analysis of bis-N7G-BD diastereomers is then performed by HPLC–ESI<sup>+</sup>–MS/MS (Figure 1). The mass spectrometer is operated in selected reaction monitoring mode by following transitions corresponding to the loss of guanine base from protonated molecules of the adduct,  $m/z$  389.1 [M +

**Table 1. Validation Results for HPLC–ESI<sup>+</sup>–MS/MS Analysis of Racemic and *meso* Forms of Bis-N7G-BD (10 fmol) Spiked into Mouse Liver DNA (0.1 mg) Using Racemic and *meso* Forms of [<sup>15</sup>N<sub>10</sub>]Bis-N7G-BD as Internal Standards**

		LOQ (10 fmol)	
		racemic	meso
day 1	mean	9.91	6.08
	RSD (%)	24	35
	accuracy (%)	99	61
	<i>n</i>	3	3
day 2	mean	10.06	9.21
	RSD (%)	18	20
	accuracy (%)	101	92
	<i>n</i>	3	3
day 3	mean	11.46	8.88
	RSD (%)	14	32
	accuracy (%)	115	89
	<i>n</i>	3	3
interday	mean	10.48	8.06
	RSD (%)	8.2	21
	accuracy (%)	105	81
	<i>n</i>	3	3

H]<sup>+</sup> → *m/z* 238.1 [M + H – Gua]<sup>+</sup>, and the formation of protonated guanine, *m/z* 389.1 [M + H]<sup>+</sup> → *m/z* 152.1 [Gua + H]<sup>+</sup> (Figure 1). <sup>15</sup>N<sub>10</sub>-labeled internal standards are analyzed analogously using the transitions *m/z* 399.1 → *m/z* 243.1 and *m/z* 399.1 → *m/z* 157.1 [M + H – Gua]<sup>+</sup>. While (*S,S*)- and (*R,R*)-bis-N7G-BD lesions (Scheme 2) are enantiomeric and thus have identical HPLC retention times (5.6–6 min, depending on the sample pH), the *meso* adducts elute slightly later from the HPLC column (*t<sub>R</sub>*, 7.3–8 min) (Figure 1). The HPLC–ESI<sup>+</sup>–MS/MS responses were linear between 10 and 1000 fmol of each adduct, with *R*<sup>2</sup> values >0.9995 (Figure 3). The method was validated by spiking control mouse liver DNA (0.1 mg) with known amounts of bis-N7G-BD isomers and the corresponding <sup>15</sup>N<sub>10</sub>-labeled internal standards. A good correlation was observed between the expected and measured levels of bis-N7G-BD in mouse liver DNA (Figure 4). Calculated amounts of racemic and *meso* forms of bis-N7G-BD at the LOQ (10 fmol) were within 20% of the theoretical value (Table 1).

The detection limits for bis-N7G-BD diastereomers (1–5 fmol for standards and 5–10 fmol for spiked mouse DNA) are not as low as those for other DNA adducts analyzed in our laboratory (subfemtomole). This difference in sensitivity may be attributed to the use of free nucleobases for bis-N7G-BD adduct analyses. Under ESI<sup>+</sup>–MS/MS conditions, nucleoside adducts fragment much more readily than free nucleobases because of the facile cleavage of the glycosidic bond and the formation of protonated nucleobases (35). Unfortunately, bis-N7G-BD nucleosides are not amenable to quantitative analysis because of the intrinsic destabilization of the glycosidic bond when the N-7 position of guanine is alkylated, which leads to partial loss of deoxyribose during sample processing (results not shown). Despite these limitations, the assay was sufficiently sensitive to detect bis-N7G-BD adducts in tissues of BD-treated laboratory mice (see below).

**In Vivo Analysis of Bis-N7G-BD.** The new quantitative HPLC–MS/MS method was employed to analyze the formation of bis-N7G-BD cross-links in DNA extracted from liver and lung tissues of C57BL/6 mice exposed to 0 or 625 ppm BD for 5 days by inhalation (Figure 5). We found that liver DNA of treated mice contained 3.17 ± 0.35 racemic adducts per 10<sup>6</sup> guanines, while the amounts of *meso*-bis-N7G-BD were below the detection limit of our method (Table 2). DNA of control animals did not contain any bis-N7G-BD lesions (Table 2). Lung DNA isolated from treated animals contained significantly lower

**Table 2. Quantitative Analysis of Racemic Bis-N7G-BD in Liver (0.1 mg) and Lung (0.05 mg) DNA of Control and BD-Exposed (625 ppm for 5 Days) C57BL/6 Mice**

sample	racemic bis-N7G-BD	<i>meso</i> -bis-N7G-BD
	adducts per 10 <sup>6</sup> guanines	adducts per 10 <sup>6</sup> guanines
liver, control ( <i>N</i> = 5)	<0.05	<0.1
liver, 625 ppm BD ( <i>N</i> = 4)	3.17 ± 0.35	<0.1
lung, control ( <i>N</i> = 4)	<0.05	<0.1
lung, 625 ppm BD ( <i>N</i> = 4)	1.79 ± 0.54	<0.1

amounts of racemic bis-N7G-BD (1.79 ± 0.54 per 10<sup>6</sup> guanines, *P* < 0.01). No *meso* lesions were detected in either tissue (Table 2). Representative HPLC–ESI<sup>+</sup>–MS/MS analysis chromatograms of a BD-exposed and control mouse DNA are shown in Figure 5.

## Discussion

Specific biomarkers of BD exposure and metabolic formation of DEB are needed to help identify the origins of interspecies differences in the sensitivity to BD carcinogenesis and to evaluate human risks associated with BD exposure. Previous in vivo analyses of DEB–DNA adducts have been limited to N7-(2',3',4'-trihydroxybut-1'-yl) guanine (THBG) (31–33), N1-THB-Ade (36), N3-THB-Ade (31), and N<sup>6</sup>-THB-Ade (37). However, more recent studies revealed that the vast majority of N7-THBG lesions (~98%) are derived from another metabolite of BD, EBD (32), suggesting that THB monoadducts cannot be used as biomarkers of DEB (30, 32, 33). In contrast, bis-N7G-BD cross-links (Scheme 2) can only be derived from DEB and therefore can be considered a specific biomarker of metabolic activation of BD to DEB.

We have developed and validated sensitive and specific methods for the quantitative analysis of bis-N7G-BD based on isotope dilution–HPLC–ESI<sup>+</sup>–MS/MS. Using our new method, the amounts of bis-N7G-BD lesions were determined in liver and lung DNA of laboratory mice exposed to 625 ppm BD for a relatively short period of time (5 days, 7 h/day). Interestingly, higher levels of bis-N7G-BD were detected in the mouse liver (3.17 adducts per 10<sup>6</sup> guanines) DNA than in the lung (1.79 adducts per 10<sup>6</sup> guanines). Our observation of DEB-induced DNA cross-links in the lung is not unexpected because mice were exposed to BD by inhalation and BD may be metabolized in the lung tissue. Higher levels of P450's responsible for the metabolism of BD to DEB are present in the liver, potentially leading to greater amounts of bis-N7G-BD cross-links in this tissue. Because DEB formed in the liver enters systemic circulation, further research is needed to determine the relative degree to which formation of this DNA-reactive intermediate in the liver versus the lung contributes to the total amount of DNA alkylation occurring in the lung. For example, Koc et al. observed similar levels of dG adducts induced by monoepoxide metabolites of BD in liver, lung, and kidney DNA of exposed mice (32). Our observation of DEB-induced DNA cross-links in mouse lung is significant because this is one of the major target tissues for BD carcinogenesis in this species (4).

The amounts of racemic bis-N7G-BD G–G cross-links found in liver DNA of BD-exposed mice (Table 2) are 4–5 fold lower than those previously reported for THBG monoadducts (33). This is consistent with the in vitro analyses of DEB-treated calf thymus DNA, which detected higher amounts of dG monoadducts as compared with bis-N7G-BD cross-links (22). Although mice form more DEB upon BD metabolism than rats do, DEB is a minor metabolite of BD in both species as compared with

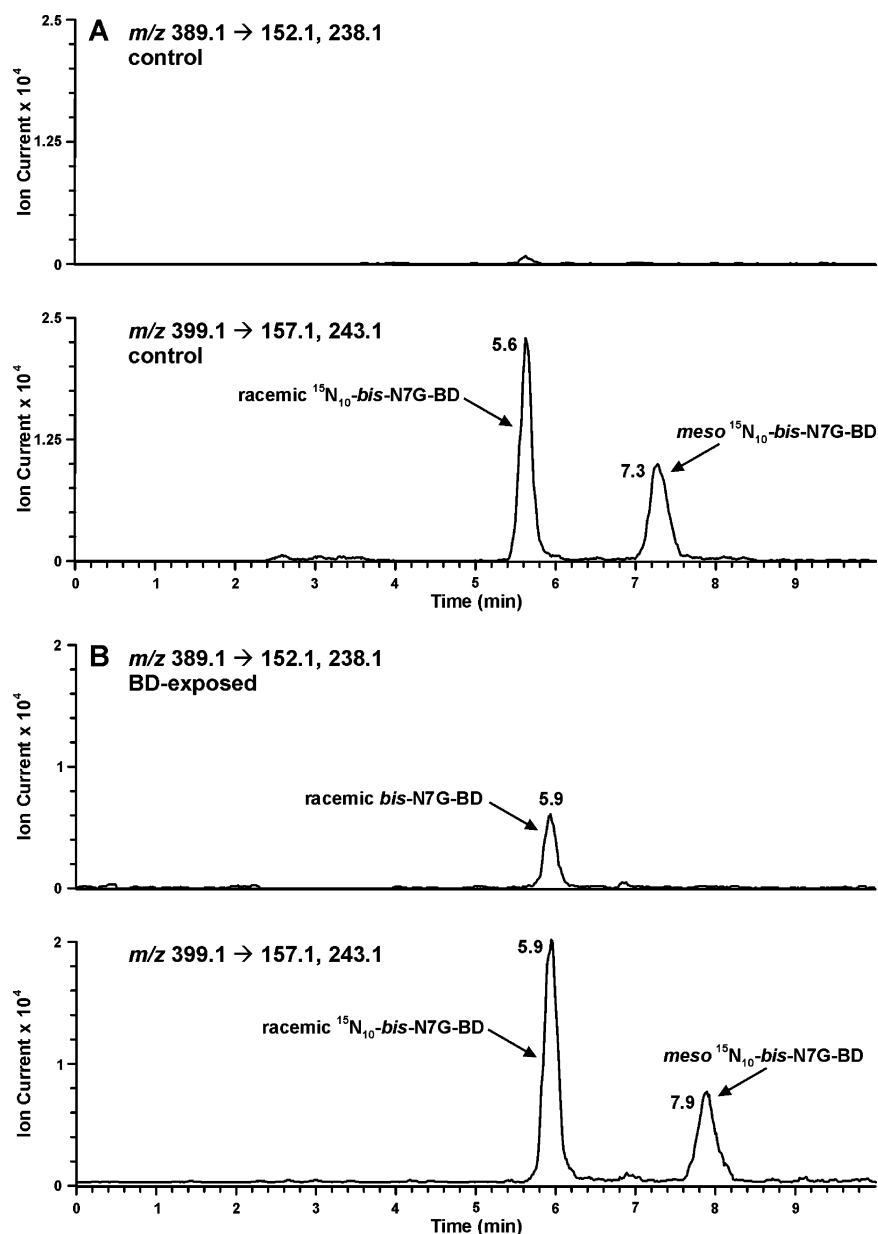


**Figure 5.** Representative HPLC–ESI<sup>+</sup>–MS/MS traces of bis-N7G-BD in liver DNA of control (A) and BD-exposed (B) mice.

much more prevalent EBD (38, 39). Therefore, our observation of significant amounts of bis-N7G-BD in liver DNA of exposed mice suggests that G–G cross-links are more stable in vivo than the corresponding monoadducts. Future studies are planned to establish the persistence of bis-N7G-BD in animal tissues.

Several explanations can be proposed for the lack of detection of *meso*-bis-N7G-BD cross-links in mouse DNA (Table 2). Because our HPLC–ESI–MS/MS method is less sensitive for the *meso* adducts as compared with racemic bis-N7G-BD, the *meso* adducts may have escaped analysis, if formed in low amounts (<5% of the total bis-N7G-BD adducts). One possibility is that BD metabolism in the mouse produces greater amounts of (*S,S*)- and (*R,R*)-diepoxides as compared with that of *meso*-DEB. For example, studies using cDNA-expressed human P450 monooxygenases have shown that individual P450's can generate *meso* and racemic forms of DEB in different molar ratios (40). In particular, P450 2A6 and 2E1 favor *meso* over racemic (2:1), whereas 2C9 forms equal levels of each (40). Alternatively, mice may detoxify *meso*-bis-N7G-BD at a faster rate than racemic bis-N7G-BD. For example, epoxide hydrolase (EH), an enzyme that detoxifies DEB by hydrolyzing

the epoxide ring to a diol (Scheme 1), has been reported to hydrolyze *meso*-DEB at a faster rate than racemic DEB (40), potentially leading to smaller amounts of *meso*-DEB available to cross-link DNA. In addition, diastereomeric bis-N7G-BD lesions may have different stabilities in DNA. Previous studies have shown that *meso*-DEB forms both interstrand and intrastrand bis-N7G-BD, whereas (*S,S*)-DEB forms specifically interstrand bis-N7G-BD (27). The half-life for spontaneous depurination of intrastrand bis-N7G-BD (35 h) is much shorter than that for interstrand bis-N7G-BD (147 h) (27). Furthermore, depending on its type, bis-N7G-BD may be processed differently by DNA repair systems. In general, interstrand lesions are expected to be more difficult to repair because they affect both strands of the DNA duplex.

To our knowledge, this method represents the first DNA-based biomarker of DEB formation upon exposure to BD. Quantitative methods for DEB-specific hemoglobin adducts, *N,N*-(2,3-dihydroxy-1,4-butanediyl)valine, have been reported (39). Although these protein adducts are specific to DEB exposure and have been used as biomarkers of BD metabolism to DEB, hemoglobin adduct levels cannot predict the amounts



of biologically relevant bifunctional DNA adducts of DEB that are formed and persist in target tissues.

The quantitative HPLC-MS/MS methods provided in this work provide the means to study accumulation, repair, and dose-response relationships of bifunctional DEB-DNA adducts in vivo. Studies are currently in progress to analyze interspecies variations in the metabolism of BD to DEB and the repair of bis-N7G-BD cross-links in BD-exposed laboratory animals. Previous investigators have noted the differences in BD metabolism by human, mouse, and rat microsomes (40, 41). In particular, mice form DEB from butadiene monoepoxide at a much faster rate than rats do (40), potentially leading to higher levels of bis-N7G-BD cross-links in the mouse. Furthermore, due to interspecies differences, there may be variations in the total amounts and the stereochemical identities of DEB generated in different species, the rates of DEB detoxification by epoxide hydrolase, and repair of bis-N7G-BD cross-links. The availability of a specific biomarker of DEB available for binding to cellular DNA will facilitate future studies that will investigate the origins of interspecies differences in susceptibility to BD-induced cancer.

**Acknowledgment.** We thank Brock Matter (University of Minnesota Cancer Center) for his assistance with the mass spectrometry experiments and Bob Carlson (University of Minnesota Cancer Center) for help with the figures for this paper. Funding for this research was from a Grant from the National Cancer Institute (R01-CA-100670). M.G. is partially supported by the University of Minnesota Transdisciplinary Tobacco Use Research Center, which is funded through the National Cancer Institute and the National Institute on Drug Abuse (Grant P50 DA 13333).

## References

- Morrow, N. L. (1990) The industrial production and use of 1,3-butadiene, *Environ. Health Perspect.* 86, 7–8.
- Pelz, N., Dempster, N. M., and Shore, P. R. (1990) Analysis of low molecular weight hydrocarbons including 1,3-butadiene in engine exhaust gases using an aluminum oxide porous-layer open-tubular fused-silica column, *J. Chromatogr. Sci.* 28, 230–235.
- Stayner, L. T., Dankovic, D. A., Smith, R. J., Gilbert, S. J., and Bailer, A. J. (2000) Human cancer risk and exposure to 1,3-butadiene—a tale of mice and men, *Scand. J. Work Environ. Health* 26, 322–330.
- Melnick, R. L., Huff, J., Chou, B. J., and Miller, R. A. (1990) Carcinogenicity of 1,3-butadiene in C57BL/6 × C3H F1 mice at low exposure concentrations, *Cancer Res.* 50, 6592–6599.
- Melnick, R. L., Shackelford, C. C., and Huff, J. (1993) Carcinogenicity of 1,3-butadiene, *Environ. Health Perspect.* 100, 227–236.
- Ward, J. B. Jr., Ammenheuser, M. M., Bechtold, W. E., Whorton, E. B. Jr., and Legator, M. S. (1994) hprt mutant lymphocyte frequencies in workers at a 1,3-butadiene production plant, *Environ. Health Perspect.* 102 (Suppl. 9), 79–85.
- Cochrane, J. E., and Skopek, T. R. (1994) Mutagenicity of butadiene and its epoxide metabolites: II. Mutational spectra of butadiene, 1,2-epoxybutene and diepoxybutane at the *hprt* locus in splenic T cells from exposed B6C3F1 mice, *Carcinogenesis* 15, 719–723.
- Melnick, R. L., and Huff, J. E. (1993) 1,3-Butadiene induces cancer in experimental animals at all concentrations from 6.25 to 8000 parts per million, *IARC Sci. Publ.*, 309–322.
- Owen, P. E., Glaister, J. R., Gaunt, I. F., and Pullinger, D. H. (1987) Inhalation toxicity studies with 1,3-butadiene. 3. Two year toxicity/carcinogenicity study in rats, *Am. Ind. Hyg. Assoc. J.* 48, 407–413.
- Henderson, R. F., Thornton-Manning, J. R., Bechtold, W. E., and Dahl, A. R. (1996) Metabolism of 1,3-butadiene: species differences, *Toxicology* 113, 17–22.
- de Meester, C. (1988) Genotoxic properties of 1,3-butadiene, *Mutat. Res.* 195, 273–281.
- Malvoisin, E., and Roberfroid, M. (1982) Hepatic microsomal metabolism of 1,3-butadiene, *Xenobiotica* 12, 137–144.
- Himmelstein, M. W., Turner, M. J., Asgharian, B., and Bond, J. A. (1996) Metabolism of 1,3-butadiene: inhalation pharmacokinetics and tissue dosimetry of butadiene epoxides in rats and mice, *Toxicology* 113, 306–309.
- Krause, R. J., and Elfarra, A. A. (1997) Oxidation of butadiene monoxide to meso- and (±)-diepoxybutane by cDNA-expressed human cytochrome P450s and by mouse, rat, and human liver microsomes: evidence for preferential hydration of meso-diepoxybutane in rat and human liver microsomes, *Arch. Biochem. Biophys.* 337, 176–184.
- Sasiadek, M., Norppa, H., and Sorsa, M. (1991) 1,3-Butadiene and its epoxides induce sister-chromatid exchanges in human lymphocytes in vitro, *Mutat. Res.* 261, 117–121.
- Cochrane, J. E., and Skopek, T. R. (1994) Mutagenicity of butadiene and its epoxide metabolites: I. Mutagenic potential of 1,2-epoxybutene, 1,2,3,4-diepoxybutane and 3,4-epoxy-1,2-butanediol in cultured human lymphoblasts, *Carcinogenesis* 15, 713–717.
- Verly, W. G., Brakier, L., and Feit, P. W. (1971) Inactivation of the T7 coliphage by the diepoxybutane stereoisomers, *Biochim. Biophys. Acta* 228, 400–406.
- Matagne, R. (1969) Induction of chromosomal aberrations and mutations with isomeric forms of L-threitol-1,4-bismethanesulfonate in plant materials, *Mutat. Res.* 7, 241–247.
- Bianchi, A., and Contin, M. (1962) Mutagenic activity of isomeric forms of diepoxybutane in maize, *J. Hered.* 53, 277–281.
- Kim, M. Y., Park, S., Tretyakova, N. Y., and Wogan, G. N. (2007) Mutagenesis of 1,2,3,4-diepoxybutane in the *supF* gene: role of stereochemistry, *Chem. Res. Toxicol.* (in press).
- Lawley, P. D., and Brookes, P. (1967) Interstrand cross-linking of DNA by difunctional alkylating agents, *J. Mol. Biol.* 25, 143–160.
- Park, S., and Tretyakova, N. (2004) Structural characterization of the major DNA-DNA cross-link of 1,2,3,4-diepoxybutane, *Chem. Res. Toxicol.* 17, 129–136.
- Millard, J. T., and White, M. M. (1993) Diepoxybutane cross-links DNA at 5'-GNC sequences, *Biochemistry* 32, 2120–2124.
- Millard, J. T., Luedtke, N. W., and Spencer, R. J. (1996) The 5'-GNC preference for mustard cross-linking is preserved in a restriction fragment, *Anticancer Drug Des.* 11, 485–492.
- Millard, J. T., and Wilkes, E. E. (2001) Diepoxybutane and diepoxy-octane interstrand cross-linking of the 5S DNA nucleosomal core particle, *Biochemistry* 40, 10677–10685.
- Millard, J. T., Hanly, T. C., Murphy, K., and Tretyakova, N. (2006) The 5'-GNC site for DNA interstrand cross-linking is conserved for diepoxybutane stereoisomers, *Chem. Res. Toxicol.* 19, 16–19.
- Park, S., Anderson, C., Loeber, R., Seetharaman, M., Jones, R., and Tretyakova, N. (2005) Interstrand and intrastrand DNA-DNA cross-linking by 1,2,3,4-diepoxybutane: role of stereochemistry, *J. Am. Chem. Soc.* 127, 14355–14365.
- Park, S., Hodge, J., Anderson, C., and Tretyakova, N. Y. (2004) Guanine-adenine cross-linking by 1,2,3,4-diepoxybutane: potential basis for biological activity, *Chem. Res. Toxicol.* 17, 1638–1651.
- Zhang, X. Y., and Elfarra, A. A. (2003) Identification and characterization of a series of nucleoside adducts formed by the reaction of 2'-deoxyguanosine and 1,2,3,4-diepoxybutane under physiological conditions, *Chem. Res. Toxicol.* 16, 1606–1615.
- Swenberg, J. A., Koc, H., Upton, P. B., Georgieva, N., Ranasinghe, A., Walker, V. E., and Henderson, R. (2001) Using DNA and hemoglobin adducts to improve the risk assessment of butadiene, *Chem.-Biol. Interact.* 135–136, 387–403.
- Tretyakova, N. Y., Chiang, S. Y., Walker, V. E., and Swenberg, J. A. (1998) Quantitative analysis of 1,3-butadiene-induced DNA adducts in vivo and in vitro using liquid chromatography electrospray ionization tandem mass spectrometry, *J. Mass Spectrom.* 33, 363–376.
- Koc, H., Tretyakova, N. Y., Walker, V. E., Henderson, R. F., and Swenberg, J. A. (1999) Molecular dosimetry of N-7 guanine adduct formation in mice and rats exposed to 1,3-butadiene, *Chem. Res. Toxicol.* 12, 566–574.
- Oe, T., Kambouris, S. J., Walker, V. E., Meng, Q., Recio, L., Werli, S., Chaudhary, A. K., and Blair, I. A. (1999) Persistence of N7-(2,3,4-trihydroxybutyl)guanine adducts in the livers of mice and rats exposed to 1,3-butadiene, *Chem. Res. Toxicol.* 12, 247–257.
- Matter, B., Malejka-Giganti, D., Csallany, A. S., and Tretyakova, N. (2006) Quantitative analysis of the oxidative DNA lesion, 2,2-diamino-4-(2-deoxy-beta-D-erythro-pentofuranosyl)amino]-5(2H)-oxazolone (oxazolone), in vitro and in vivo by isotope dilution-capillary HPLC-ESI-MS/MS, *Nucleic Acids Res.* 34, 5449–5460.
- Chaudhary, A. K., Nokubo, M., Reddy, G. R., Yeola, S. N., Morrow, J. D., Blair, I. A., and Marnett, L. J. (1994) Detection of endogenous malondialdehyde-deoxyguanosine adducts in human liver, *Science* 265, 1580–1582.
- Zhao, C., Vodicka, P., Sram, R. J., and Hemminki, K. (2001) DNA adducts of 1,3-butadiene in humans: Relationships to exposure, GST genotypes, single-strand breaks, and cytogenetic end points, *Environ. Mol. Mutagen.* 37, 226–230.
- Koivisto, P., Kilpelainen, I., Rasanen, I., Adler, I. D., Pacchierotti, F., and Peltonen, K. (1999) Butadiene diepoxide- and diepoxybutane-derived DNA adducts at N7- guanine: a high occurrence of diepoxide-

- oxide-derived adducts in mouse lung after 1,3-butadiene exposure, *Carcinogenesis* 20, 1253–1259.
- (38) Filser, J. G., Hutzler, C., Meischner, V., Veereshwarayya, V., and Csanady, G. A. (2007) Metabolism of 1,3-butadiene to toxicologically relevant metabolites in single-exposed mice and rats, *Chem.-Biol. Interact.* 166, 93–103.
- (39) Boysen, G., Georgieva, N. I., Upton, P. B., Jayaraj, K., Li, Y., Walker, V. E., and Swenberg, J. A. (2004) Analysis of diepoxide-specific cyclic N-terminal globin adducts in mice and rats after inhalation exposure to 1,3-butadiene, *Cancer Res.* 64, 8517–8520.
- (40) Kemper, R. A., Krause, R. J., and Elfarra, A. A. (2001) Metabolism of butadiene monoxide by freshly isolated hepatocytes from mice and rats: different partitioning between oxidative, hydrolytic, and conjugation pathways, *Drug Metab. Dispos.* 29, 830–836.
- (41) Elfarra, A. A., Krause, R. J., and Kemper, R. A. (2001) Cellular and molecular basis for species, sex and tissue differences in 1,3-butadiene metabolism, *Chem.-Biol. Interact.* 135-136, 239–248.

TX700020Q